Journal of Nanofluids
Vol. 4, pp. 271–292, 2015
(www.aspbs.com/jon)

MHD Convection of Nanofluids: A Review

Ali J. Chamkha[1,*], Sofen Kumar Jena[2,3], and Swarup Kumar Mahapatra[4]

[1]*Mechanical Engineering Department, Prince Mohammad Bin Fahd University (PMU), Al-Khobar 31952, Kingdom of Saudi Arabia*
[2]*Cardiovascular Innovation Institute, Department of Cardiovascular and Thoracic Surgery, School of Medicine, University of Louisville, KY 40202, USA*
[3]*Department of Mechanical Engineering, Eastern Academy of Science and Technology, Bhubaneswar 754001, India*
[4]*School of Mechanical Sciences, Indian Institute of Technology Bhubaneswar, Bhubaneswar 751013, India*

Many researchers have reported significant enhancement of nanofluids' thermal properties due to the suspension of modest nanoparticle concentrations in low thermal conductivity base fluids. Most of the nanofluids literature concentrates on the development and understanding of nanofluids properties models and their behavior as heating or cooling mechanisms in many industrial, engineering and technological applications. In the past decade, a lot of work has been done on MHD convective flow of nanofluids, but the review of these types of flow and heat transfer situations is absent from the literature till date. This paper reviews some of the available nanofluids physical properties models and focuses on presenting the various research work done on MHD convection of nanofluids in various geometries and applications.

KEYWORDS: Nanofluids, Thermal Conductivity, Viscosity, Electrical Conductivity, MHD Effects, Convection.

REVIEW

CONTENTS

1. INTRODUCTION

The word "nano" dates back to 1915 in the book "The world of neglected dimensions" by Oswald.[1] A unique feature of the matter at nano-scale makes nanotechnology a hot research area in the 21st century. In last few decades, scientists and researchers around the globe tried to continuously work on various aspects of nanotechnology. Nanofluid dynamics is one of the vital branches of research in nanotechnology nowadays. An effort has been provided in the preceding section to give a state of art review on time-wise development and applications of nanofluids.

Engineers and scientists have provided enormous efforts to enhance the heat transfer in natural convection processes in the past two century; this process captured the attention of the research community around the globe after Maxwell[2] who provided his theory in 1873. Poor thermal conductivity of traditional fluids like oil, water and organic liquid makes these fluids unsuitable to use in heat transfer devices, where higher heat transfer is expected. Gradually in the early 20th century, scientists started dispersing millimeter to micron-order conducting particles in classical fluids to enhance the heat transfer. However, rapid sedimentation of these particles minimizes the use of this kind of mixture in heat transferring devices. Further, the size of these suspensions induces additional resistance and causes erosion. Gradually, the science community looked for a particle dimension which is not affected by the gravity action. Rapid development of instrumentation science helped to break the particles to nano-scale where the matter posses unique physical and chemical properties. The modern science has provided the opportunity to prepare material in the size of 50 nm. Nanoparticles also exist in nature in the form of ultra-fine suspensions. Nanoparticles of different materials are produced by different physical and chemical synthesis processes. Mechanical grinding and inert gas condensation method for preparation of nanoparticle are discussed by Granquist and Buhrman.[3] For the first time, Choi[4,5] of Argonne National Laboratory named the emulsion of these particulate matters of particle size in the order of nanometers as nanofluids. Later, Eastman et al.[6] has discussed the enhancement of heat transfer through the use nanofluids. Nano-metallic particulate suspension in a base fluid makes it suitable and

*Author to whom correspondence should be addressed.
Email: achamkha@pmu.edu.sa
Received: 10 March 2015
Accepted: 26 March 2015

superior in terms of heat transfer compared to conventional liquids. The abrasion related properties of a nanofluid are found to be excellent over the traditional fluid-solid mixture. The whole world was searching for micro machines and their applications after the historical lecture of the celebrated physicist Richard Feynman in 1959 during the American Physical Society meeting. In the last decades of the 20th century, recognition of these unique properties of nanofluids made it possible to design and to fabricate ultra-light and compact heat transfer equipment. For the first time, a decade of research in nanofluids around the globe was placed in the literature review of Keblinski et al.[7] At that time, theoretical knowledge for complete understanding of the mechanisms involved in the transport process was blurred. In the subsequent years, Wang and Mazumdar[8] have provided a state of art literature review on the characterization of nanofluids, in both experimental and theoretical prospective. A detailed description about the experimental techniques involved in the process of a nanofluid preparation is placed in the classical review article of Wang and Mazumdar.[8] The development and works on nanofluids have taken position in the contemporary review literature of Das et al.[9] and Trisaksri and Wongwises.[10] Contemporary fundamental issues on the convection of nanofluids are highlighted in the above review articles. In the last decades, significant amount of experimental and numerical works has been done on nanofluids. The objective of the present review article is to illustrate the basic mechanisms of heat transfer in MHD flow of nanofluid, to show various models to evaluate the properties of MHD flow in nanofluid and present the numerical works on MHD transport of nanofluid that have been done in the past decade.

When solid nanoparticles with a typical length scale 1–100 nm are suspended in a base fluid, the effective thermal conductivity and heat transfer coefficient of the mixture become enhanced compared to that of the base fluid. Keeping in mind the homogeneity, optimal pumping power, long term stability, minimum clogging and high thermal conductivity, normally Cu, CuO, SiO, TiO_2 and

REVIEW

Ali J. Chamkha is Professor and Chairman of the Mechanical Engineering Department at the Prince Mohammad Bin Fahd University (PMU) in the Kingdom of Saudi Arabia. He earned his Ph.D. in Mechanical Engineering from Tennessee Technological University, USA, in 1989. His research interests include multiphase fluid-particle dynamics, nanofluids dynamics, fluid flow in porous media, heat and mass transfer, magnetohydrodynamics and fluid-particle separation. He has served as an Associate Editor for many journals such as International Journal of Numerical Method for Heat and Fluid Flow, Journal of Applied Fluid Mechanics, International Journal for Microscale and Nanoscale Thermal and Fluid Transport Phenomena and he is currently the Deputy Editor-in-Chief for the International Journal of Energy and Technology. He has authored and co-authored over 450 publications in archival international journals and conferences.

Sofen Kumar Jena is working as a postdoctoral researcher in Cardiovascular Innovation Institute, Department of Cardiovascular and Thoracic Surgery, School of Medicine, University of Louisville, USA. He has received his Ph.D. in Mechanical Engineering from Jadavpur University, Kolkata, India in the year 2014. In the past, he worked as a junior research fellow in the School of Mechanical Sciences, Indian Institute of Technology Bhubaneswar, India, visiting research scholar at Fraunhofer ITWM, Kaiserslautern, Germany and as Assistant Professor, Department of Mechanical Engineering, Eastern Academy of Science and Technology, Bhubaneswar, India. His research interests include magnetohydrodynamics, conjugate heat and mass transfer, flow in porous media, double diffusion, non-Newtonian flow, thermal radiation modeling and biological fluid dynamics. He has authored and co-authored over twenty publications in archival international journals and conferences.

Swarup Kumar Mahapatra is working as Professor and Head, School of Mechanical Sciences, Indian Institute of Technology Bhubaneswar, India. He has 25 years of teaching and research experience. He is involved in many research projects. His research interests are computational fluid dynamics, conjugate heat transfer, and radiative heat transfer modeling. In addition, he is working on the development of mathematical model for transient radiative heat transfer for its application in the field of bio-heat transfer. He received his Ph.D. from Jadavpur University, India, in 2000. He has also organized many conferences and short-term courses in his field of research. He has authored and co-authored over seventy publications in archival international journals and conferences.

Al_2O_3 are used as nanoparticles. The thermal conductivities of metallic solid particles, non-metallic solid particles and base fluids are provided in Table I. In last two decade, researchers like Masuda et al.,[11] Lee et al.,[12] Xuan and Li[13] and Xuan and Roetzel[14] have shown that for a low particle concentration within 1–5%, the thermal conductivity of the nanofluid enhanced more than 20%. Eastman et al.[6] have reported 60% enhancement in thermal conductivity with the use of 5% CuO nanoparticles with water as a base fluid. Choi et al.[15] have shown that the thermal conductivity of a nanofluid becomes doubled with the addition of less than 1% nanoparticles. Gradually, scientists around the globe looked for a theoretical explanation of enhancement of heat transfer of nanofluids and gradually different models for nanofluids came into the picture. This will be explained in the next section.

2. HYDRODYNAMIC MODELS FOR NANOFLUID FLOW

Two types of models have been used for nanofluid flow in the literature. These are the single-phase and the two-phase approach. In the two-phase approach, the base fluid is considered as a continuous phase and the suspended particles are taken as a continuous/discrete phase and the classical Euler–Euler and Euler–Lagrange approaches are used for the simulation of flow. The two-phase model accounts for the no slip conditions between the particles and the base fluid and several other factors like Brownian motion, solid-fluid friction, gravitational sedimentation, Brownian diffusion and dispersion for the particulate matter. Research on nanofluid flow considering the two-phase model has appeared in the work of Mirmasoumi and Behzadmehr,[16] Bianco et al.,[17] Akbarinia and Laur.[18] The two-phase model for a nanofluid is computationally more expensive and keeping the size of the solid particle in view, the authentication of the conventional two-phase model for a nanofluid is questionable. The literature is also silent on the same. Several other contemporary works tried to reproduce the flow of a nanofluid as a single-phase fluid motion.

Table I. Thermal conductivities of various solid and liquids (Wang and Majumdar).[8]

Solid/Liquids	Materials	Thermal conductivity (W/m K)
Metallic solids	Silver	429
	Copper	401
	Aluminum	237
Non-metallic solids	Diamonds	3300
	Carbon nanotubes	3000
	Silicon	148
	Alumina (Al_2O_3)	40
Metallic liquids	Sodium @ 644K	72.3
Non-metallic liquids	Water	0.613
	Ethylene glycol (EG)	0.253
	Engine oil	0.145

Because of the small particle size and the low concentration of the nanoparticles, the base fluid is assumed to be a homogeneous mixture of the suspended particles. In the single-phase fluid, the slip velocity between the fluid and the solid particles are taken into account, which means that the suspended solid particles move with the same velocity as that of the fluid. Also, the suspended particles are assumed to be in thermal equilibrium with the base fluid. Abu-Nada et al.,[19,20] Abouali and Falahatpisheh[21] have used the single-phase model for the flow of nanofluids. This single-fluid approach is found to be suitable for the flow of a nanofluid as it produces results that agree with the experimental data in some cases. The simple computational implementation of the single-phase approach makes it more popular among the researchers. In the single-phase approach, the hydrodynamics equations for a nanofluid flow are analogous to the equations for a base fluid flow, i.e., the same momentum, energy conservation and continuity equations are valid for a nanofluid flow, except the properties of the fluid. The hydrodynamic equations for the nanofluid are expressed as

$$\nabla \cdot \vec{V} = 0 \tag{1}$$

$$\rho_{\mathrm{nf}} \frac{D\vec{V}}{Dt} = \nabla p + \mu_{\mathrm{nf}} \nabla \cdot (\nabla \vec{V} + \nabla \vec{V}^T) + f \tag{2}$$

$$(\rho C_p)_{\mathrm{nf}} \frac{DT}{Dt} = \nabla (k_{\mathrm{nf}} \nabla T) \tag{3}$$

where ρ_{nf}, μ_{nf}, $\rho C_{p_{\mathrm{nf}}}$, k_{nf} represent the density, viscosity, specific heat capacity and the thermal conductivity of the nanofluid, respectively. Vital research on nanofluids has been done in the process of evaluation of these properties. Many experimental and theoretical works come into picture explaining these properties in their prospective. Each theory and model has its own advantages and limitations. However, any universal acceptable model is not available which is unique for every operating condition. In the subsequent section, a detailed description has been given regarding the development of the model, its suitability and limitations.

2.1. Density

The density of a nanofluid is evaluated taking the volume fraction of the suspended nanoparticles and keeping the density of both the base fluid and the nanoparticles into account. In mathematical form, this is expressed as

$$\rho_{\mathrm{nf}} = \phi \rho_p + (1 - \phi) \rho_f \tag{4}$$

2.2. Specific Heat Capacity

Mathematically, the specific heat of a nanofluid is expressed by two formulations. Pak and Cho,[22] Maïga et al.[23] and Palm et al.[24] have taken Eq. 5(a), for heat capacity in their research work.

$$(C_p)_{\mathrm{nf}} = \phi (C_p)_p + (1 - \phi)(C_p)_f \tag{5a}$$

REVIEW

Researchers like Eastman et al.,[25] Das et al.[26] have taken the specific heat capacity of the nanofluid as expressed by Eq. 5(b) in their studies.

$$(\rho C_p)_{\mathrm{nf}} = \phi(\rho C_p)_p + (1-\phi)(\rho C_p)_f \tag{5b}$$

The above two equations for specific heat and specific heat capacity of nanofluids produce two different results. Because of lack of experimental validation to prove the uniqueness of each model, both models are considered to be equivalent to each other (Xuan and Roetzel).[14]

2.3. Thermal Conductivity

In general practices, highly conducting metallic nanoparticles are added to the low conductive base fluids to improve the overall conductivity of the nanofluids. A lot of correlations are available to evaluate the thermal conductivity of the nanofluids. These correlations examined the enhancement of the thermal conductivity of a nanofluid compared to that of the base fluid due to the addition of nanoparticles. The models are classified into two categories, i.e., static model and dynamics model. The static model accounts only for the thermal conductivity of the base fluid, nanoparticles and the volume fraction of nanoparticles for determination of the thermal conductivity of nanofluids. Few of the important correlations for equivalent thermal conductivity of nanofluids are described below.

Maxwell[2] proposed the equivalent thermal conductivity of a mixture consisting of continuous base fluid and discrete solid particles from his classical research on conduction through heterogeneous materials. Mathematically, the same is expressed as

$$\frac{k_{\mathrm{nf}}}{k_f} = \frac{k_p + 2k_f - 2\phi(k_f - k_p)}{k_p + 2k_f + \phi(k_f - k_p)} \tag{6a}$$

The Maxwell model is a deterministic and efficient one but the limitation of the Maxwell model is that, it assumes the discontinuous solid particles are spherical in size. The Maxwell theory largely fails when applied to nanofluids. It either under estimates or over estimates the effective thermal conductivity depending upon the size of the suspended particles being either small or large, respectively.

Bruggeman[27] has provided a model for the thermal conductivity of a nanofluid considering the shape of the nanoparticles. Mathematically, it is expressed as

$$\frac{k_{\mathrm{nf}}}{k_f} = \frac{(3\phi-1)\frac{k_p}{k_f} + [3(1-\phi)-1] + \sqrt{\Delta_B}}{4}$$

$$\Delta_B = \left[(3\phi-1)\frac{k_p}{k_f} + (3(1-\phi)-1)\right]^2 + \frac{8k_p}{k_f} \tag{6b}$$

Production of perfect spheroids during mechanical grinding and decomposition process is not possible. Hence, later Hamilton and Crosser[28] considered the particle shape factor for determining the thermal conductivity of a nanofluid. Mathematically, their model is expressed as

$$\frac{k_{\mathrm{nf}}}{k_f} = \frac{k_p + (n-1)k_f - (n-1)\phi(k_f - k_p)}{k_p + (n-1)k_f + \phi(k_f - k_p)} \tag{6c}$$

where n represents the particle shape factor which is related to sphericity (ψ) by the function $n = 3/\psi$. The sphericity is the ratio of the surface areas of the particle to the sphere which has the same volume with that of the particle. The Hamilton-Crosser model[28] reduces to the Maxwell model[2] for $\psi = 1$. Experimentally, the Hamilton-Crosser model is found to be correct for a mixture where the thermal conductivity of suspended particles is 100 times the thermal conductivity of the base fluid with a suspension volume fraction less than 30%. Jeffrey[29] has provided his model for the thermal conductivity of a nanofluid for spherical suspensions. This model mathematically takes higher order terms into account and more precisely calculates the thermal conductivity of nanofluids. This is expressed as

$$\frac{k_{\mathrm{nf}}}{k_f} = 1 + 3\left(\frac{k_p/k_f - 1}{k_p/k_f + 1}\right)\phi + \left(3\left(\frac{k_p/k_f - 1}{k_p/k_f + 1}\right)^2 + \frac{3}{4}\left(\frac{k_p/k_f - 1}{k_p/k_f + 1}\right)^2 + \frac{9}{16}\left(\frac{k_p/k_f - 1}{k_p/k_f + 1}\right)^3 \times \left(\frac{k_p/k_f + 1}{2k_p/k_f + 3}\right)\ldots\right)\phi^2 \tag{6d}$$

Davis[30] provided a model which accounts for the interaction effect among the randomly dispersed spheres and is expressed as

$$\frac{k_{\mathrm{nf}}}{k_f} = 1 + \left(\frac{3(k_p/k_f - 1)\phi}{(k_p/k_f + 2) - (k_p/k_f - 1)\phi}\right)(\phi + f(k_p/k_f)\phi^2) \tag{6e}$$

Lu and Lin[31] provided a model for the thermal conductivity which accounts for both spherical and non-spherical particles as follows:

$$\frac{k_{\mathrm{nf}}}{k_f} = 1 + (k_p/k_f)\phi + b\phi^2 \tag{6f}$$

Yu and Choi[32] have modified the Maxwell model with the assumption that the base fluid molecules surrounding the nanoparticles formed a solid equivalent layer. This nano-layer works as a bridge between the solid nanoparticle and the base fluid (see Fig. 1) and enhances the thermal conductivity of the nanofluids. Mathematically, this is expressed as

$$\frac{k_{\mathrm{nf}}}{k_f} = \frac{k_p + 2k_f - 2\phi(k_f - k_p)(1+\beta)^3}{k_p + 2k_f + \phi(k_f - k_p)(1+\beta)^3} \tag{6g}$$

Patel et al.[33] have provided a model which accounts for the thermal diffusivity and viscosity along with the particle

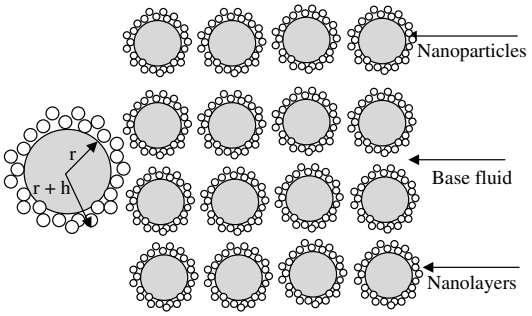

Fig. 1. Structures of nanofluid discussed by Yu and Choi.[32]

diameter to calculate the effective thermal conductivity of nanofluids. Mathematically, this is given by

$$\frac{k_{\mathrm{nf}}}{k_f} = 1 + \frac{k_p d_f \phi}{k_f d_p (1-\phi)}\left[1 + c\frac{2k_B T d_p}{\pi \alpha_f \mu_f d_p^2}\right] \quad (6\mathrm{h})$$

Mintsa et al.[34] have provided a temperature-dependant thermal conductivity model for water-based nanofluids, which is expressed as

$$\frac{k_{\mathrm{nf}}}{k_f} = 1.72\phi + 1 \quad (6\mathrm{i})$$

The models discussed above are based on the static model to determine the thermal conductivity of a nanofluid. The thermal conductivity of nanofluids in motion is different from that of the thermal conductivity of nanofluids at rest. In the dynamic model, the Brownian motion induces a micro-mixing effect and augmented conduction due to nanoparticle clustering which are taken into consideration to evaluate the equivalent thermal conductivity. A lot of correlations on the dynamic thermal conductivity of nanofluids have been developed in the past decades. Few classical correlations are discussed below.

Koo and Kleinstreuer[35] have provided a dynamical model for the thermal conductivity of a nanofluid, which takes the temperature, density and specific heat of the base fluid as well as the particle size into consideration. This is expressed as

$$\frac{k_{\mathrm{nf}}}{k_f} = \frac{k_p + 2k_f - 2\phi(k_f - k_p)}{k_p + 2k_f + \phi(k_f - k_p)} + 5\times 10^4 \beta \phi \rho_f (C_p)_f \sqrt{\frac{k_B T}{d_p \rho_p}} f(T, \phi) \quad (6\mathrm{j})$$

This model mathematically splits the total thermal conductivity of the nanofluid into a static part and a Brownian movement part. The traditional Maxwell[2] model is used to find out the static thermal conductivity which is expressed as the first term of Eq. (6j). The second term of Eq. (6j) represents the mathematical correlation to determine the thermal conductivity due to the Brownian movement of the nanoparticles. Prasher[36] has taken the random particle motion effect of a multi-sphere Brownian model to predict the thermal conductivity of a nanofluid, which is expressed as

$$\frac{k_{\mathrm{nf}}}{k_f} = (1 + A\mathrm{Re}^m \mathrm{Pr}^{0.333}\phi) \times \left(\frac{[k_p(1+2Bi)+2k_m]+2\phi[k_p(1-2Bi)-k_m]}{[k_p(1+2Bi)+2k_m]-\phi[k_p(1-2Bi)-k_m]}\right) \quad (6\mathrm{k})$$

where Re and Pr and Bi are the Reynolds, Prandtl and the nanoparticle Biot numbers, respectively and A and m are empirical constants.

Considering the four modes of energy transport to incorporate the Brownian motion effect, Jang and Choi[37] have provided a model for the equivalent thermal conductivity as

$$\frac{k_{\mathrm{nf}}}{k_f} = (1-\phi) + \phi\frac{k_p}{k_f} + 3C_1\frac{d_{\mathrm{bf}}}{d_p}\mathrm{Re}_{\mathrm{dp}}\,\mathrm{Pr}\,\phi \quad (6\mathrm{l})$$

where d_{bf} represents the base fluid molecular diameter, d_p and $\mathrm{Re}_{\mathrm{dp}}$ represents the particle diameter and the Reynolds number, respectively. Li[38] modified the Koo and Kleinstreuer[35] model to account for the particle diameter, temperature and the volume fraction through a g-function. This model is known as the KKL (Koo-Kleinstreuer-Li) model for the equivalent dynamic thermal conductivity of a nanofluid.

$$k_{\mathrm{brownian}} = 5\times 10^4 \phi (\rho C_p)_f \sqrt{\frac{k_B T}{d_p \rho_p}} g(T, \phi, d_p)$$

$$g(T, \phi, d_p) = (a + b\ln(d_p) + c\ln(\phi) + d\ln(\phi)\ln(d_p) + e\ln(d_p)^2)\ln(T) + (g + h\ln(d_p) + i\ln(\phi) + j\ln(\phi)\ln(d_p) + k\ln(d_p)^2) \quad (6\mathrm{m})$$

where the coefficients a–k are depend upon the particle fluid pairing.

All of the models discussed above for evaluation of the thermal conductivity of nanofluids are problem specific. The static models normally over predict the effective thermal conductivity while the dynamics conditions are validated for particular cases. Any universal model is not accepted to fit for every situation of a nanofluid flow. Hence, the development of equivalent models for nanofluids is still a hot topic of research around the globe.

2.4. Dynamic Viscosity

The thermal conductivity enhancement is not the sole noteworthy effect that arises because of the suspension of the nanoparticles in a base fluid. Simultaneously, the dynamic viscosity of the nanofluid changes with the inclusion of these suspended particles, hence, the fluid motion drastically decreases. Calculation of the effective dynamic viscosity of a nanofluid is a crucial job. A lot of empirical correlations are available in the literature, which develop the model to calculate the dynamic viscosity of

REVIEW

a nanofluid using various theoretical and experimental studies. Classical models for the dynamic viscosity calculations are explained below.

The Brinkman[39] model for the dynamic viscosity ratio of a nanofluid to a base fluid is expressed as

$$\frac{\mu_{\rm nf}}{\mu_f} = \frac{1}{(1-\phi)^{2.5}} \tag{7a}$$

The Einstein[40] model for the dynamic viscosity is valid for $\phi < 0.05$ and is expressed as

$$\frac{\mu_{\rm nf}}{\mu_f} = (1+2.5\phi) \tag{7b}$$

The Brinkman[39] and the Einstein[40] models underestimate the dynamic viscosity of a nanofluid. In the last decade, researchers around the globe provided few more models to calculate the dynamic viscosity. As these models are based on a small number of experimentations, hence, their universal validity is somehow limited. Some of the important models are discussed below.

Pak and Cho[22] model

$$\frac{\mu_{\rm nf}}{\mu_f} = (1+39.11\phi+533.9\phi^2) \tag{7c}$$

Koo and Kleinstreuer[35] model

$$\begin{aligned}
&\mu_{\rm nf} = 5\times10^4\beta\phi\rho_f\sqrt{\frac{k_B T}{d_p\rho_p}}f(T,\phi)\\
&\beta = 0.0137(100\phi)^{-0.8229} \quad \forall\phi<1\%\\
&\beta = 0.0011(100\phi)^{-0.7272} \quad \forall\phi>1\%\\
&f(T,\phi) = (-6.04\phi+0.4705)T\\
&\qquad +(1722.3\phi-134.63)\\
&1\%\le\phi\le4\%, 300\ {\rm K}\le T\le325\ {\rm K}
\end{aligned} \tag{7d}$$

Maïga et al.[41] model

$$\frac{\mu_{\rm nf}}{\mu_f} = (1+7.3\phi+123\phi^2) \tag{7e}$$

Orozco[42] Brownian model

$$\frac{\mu_{\rm nf}}{\mu_f} = (1+2.5\phi+6.17\phi^2) \tag{7f}$$

Nguyen et al.[43] model

$$\begin{aligned}
\mu_{\rm CuO} = {} & -0.6967+\frac{15.937}{T}+1.238\phi+\frac{1556.14}{T^2}\\
& -0.259\phi^2-30.88\frac{\phi}{T}-\frac{19652.74}{T^3}+0.01593\phi^3\\
& +4.38206\frac{\phi^2}{T}+147.573\frac{\phi}{T^2}
\end{aligned} \tag{7g}$$

$$\begin{aligned}
\mu_{\rm Al_2O_3} = {} & \exp(3.003-0.04203T-0.5445\phi+0.0002553T^2\\
& +0.0524\phi^2-1.622\phi^{-1})
\end{aligned}$$

Jang et al.[44] model

$$\frac{\mu_{\rm nf}}{\mu_f} = (1+2.5\phi)\left[1+\eta\left(\frac{d_p}{H}\right)^{-3\varepsilon}\phi^{2/3}(1+\varepsilon)\right] \tag{7h}$$

Nguyen et al.[45] model

$$\frac{\mu_{\rm nf}}{\mu_f} = (1+0.025\phi+0.015\phi^2) \tag{7i}$$

Gherasim et al.[46] model

$$\frac{\mu_{\rm nf}}{\mu_f} = 0.904e^{14.8\phi} \tag{7j}$$

2.5. Electrical Conductivity

In the available literature, only two models for determining the electrical conductivity of an electrically-conducting nanofluid is available. Aminossadati et al.[47] have used the following model for determining the electrical conductivity of nanofluids:

$$\frac{\sigma_{\rm nf}}{\sigma_f} = (1-\phi)+\phi\frac{\sigma_p}{\sigma_f} \tag{8a}$$

The latest correlation for computing the electrical conductivity of a nanofluid is discussed in the works of Mahmoudi et al.[48] and Sheikholeslami et al.[49] Mathematically, this is expressed as

$$\frac{\sigma_{\rm nf}}{\sigma_f} = 1+\frac{3(\gamma-1)\phi}{(\gamma+2)-(\gamma-1)\phi} \quad \gamma=\frac{\sigma_p}{\sigma_f} \tag{8b}$$

For convenience, all the properties of a nanofluid discussed above are presented in a tabular form in Table II.

2.6. Applications Work of Nanofluids

In the past one and half decades, a lot of theoretical, numerical and experiential works have been done on nanofluids applications. A state of the art literature on the classical works of nanofluids is discussed in the review works of Das et al.,[9] Wang and Mujumdar[8] and Trisaksri, and Wongwises.[10] Kakaç and Pramuanjaroenkij[50] have provided a review on convective heat transfer enhancement with nanofluids. Paul et al.[51] have narrated the techniques of measuring the thermal conductivity of nanofluids in their review of literature. Kleinstreuer and Feng,[52] Corcione[53] and Ghadimi at al.[54] have provided literature reviews on various models for determining the properties of nanofluids. Haddad et al.[55] have discussed the recent works on applications of nanofluids in their review paper. Mahian et al.[56] have provided a review on the applications of nanofluids for solar energy. All the works discussed above covered the works on nanofluids in the past two decades. However, a lot of works on MHD flow and heat transfer of nanofluids have been done in the past decades. The current study gives a review on MHD flow and heat transfer of nanofluids in the past five years.

Table II. Models for evaluation of properties of nanofluids.

Sl no.	Models	Mathematical expressions
		Thermal conductivity
1.	Maxwell[2]	$\frac{k_{nf}}{k_f}=\frac{k_p+2k_f-2\phi(k_f-k_p)}{k_p+2k_f+\phi(k_f-k_p)}$
2.	Bruggeman[27]	$\frac{k_{nf}}{k_f}=\frac{(3\phi-1)k_p/k_f+[3(1-\phi)-1]+\sqrt{\Delta_B}}{4}$ $\Delta_B=[(3\phi-1)k_p/k_f+(3(1-\phi)-1)]^2+\frac{8k_p}{k_f}$
3.	Hamilton and Crossover[28]	$\frac{k_{nf}}{k_f}=\frac{k_p+(n-1)k_f-(n-1)\phi(k_f-k_p)}{k_p+(n-1)k_f+\phi(k_f-k_p)}$
4.	Jeffrey[29]	$\frac{k_{nf}}{k_f}=1+3\left(\frac{k_p/k_f-1}{k_p/k_f+1}\right)\phi+\left(3\left(\frac{k_p/k_f-1}{k_p/k_f+1}\right)^2+\frac{3}{4}\left(\frac{k_p/k_f-1}{k_p/k_f+1}\right)^2+\frac{9}{16}\left(\frac{k_p/k_f-1}{k_p/k_f+1}\right)^3\left(\frac{k_p/k_f+1}{2k_p/k_f+3}\right)\cdots\right)\phi^2$
5.	Davis[30]	$\frac{k_{nf}}{k_f}=1+\left(\frac{3(k_p/k_f-1)\phi}{(k_p/k_f+2)-(k_p/k_f-1)\phi}\right)(\phi+f(k_p/k_f)\phi^2)$
6.	Lu and Lin[31]	$\frac{k_{nf}}{k_f}=1+(k_p/k_f)\phi+b\phi^2$
7.	Yu and Choi[32]	$\frac{k_{nf}}{k_f}=\frac{k_p+2k_f-2\phi(k_f-k_p)(1+\beta)^3}{k_p+2k_f+\phi(k_f-k_p)(1+\beta)^3}$
8.	Patel et al.[33]	$\frac{k_{nf}}{k_f}=1+\frac{k_pd_f\phi}{k_fd_p(1-\phi)}\left[1+c\frac{2k_BTd_p}{\pi\alpha_f\mu_fd_p^2}\right]$
9	Mintsa et al.[34]	$\frac{k_{nf}}{k_f}=1.72\phi+1$
10.	Koo and Kleinstreuer[35]	$\frac{k_{nf}}{k_f}=\frac{k_p+2k_f-2\phi(k_f-k_p)}{k_p+2k_f+\phi(k_f-k_p)}+5\times10^4\beta\phi\rho_f(C_p)_f\sqrt{\frac{k_BT}{d_p\rho_p}}f(T,\phi)$
11.	Prasher[36]	$\frac{k_{nf}}{k_f}=(1+ARe^m\mathrm{Pr}^{0.333}\phi)\times\left(\frac{[k_p(1+2Bi)+2k_m]+2\phi[k_p(1-2Bi)-k_m]}{[k_p(1+2Bi)+2k_m]-\phi[k_p(1-2Bi)-k_m]}\right)$
12.	Jang and Choi[37]	$\frac{k_{nf}}{k_f}=(1-\phi)+\phi\frac{k_p}{k_f}+3C_1\frac{d_{bf}}{d_p}\mathrm{Re}_{dp}\,\mathrm{Pr}\,\phi$
13.	Koo-Kleinstreuer-Li[38]	$k_{brownian}=5\times10^4\phi(\rho C_p)_f\sqrt{\frac{k_BT}{d_p\rho_p}}g(T,\phi,d_p)$ $g(T,\phi,d_p)=(a+b\ln(d_p)+c\ln(\phi)+d\ln(\phi)\ln(d_p)+e\ln(d_p)^2)\ln(T)+(g+h\ln(d_p)+i\ln(\phi)+j\ln(\phi)\ln(d_p)+k\ln(d_p)^2)$
		Dynamic viscosity
1.	Brinkman[39]	$\frac{\mu_{nf}}{\mu_f}=\frac{1}{(1-\phi)^{2.5}}$
2.	Einstein[40]	$\frac{\mu_{nf}}{\mu_f}=(1+2.5\phi)$
3.	Pak and Cho[22]	$\frac{\mu_{nf}}{\mu_f}=(1+39.11\phi+533.9\phi^2)$
4.	Koo and Kleinstreuer[35]	$\mu_{nf}=5\times10^4\beta\phi\rho_f\sqrt{\frac{k_BT}{d_p\rho_p}}f(T,\phi)$ $\beta=0.0137(100\phi)^{-0.8229}\forall\,\phi<1\%$ $\beta=0.0011(100\phi)^{-0.7272}\forall\,\phi>1\%$ $f(T,\phi)=(-6.04\phi+0.4705)T+(1722.3\phi-134.63)$ $1\%\le\phi\le4\%,\ 300\ \mathrm{K}\le T\le325\ \mathrm{K}$

REVIEW

Table II. Continued.

Sl no.	Models	Mathematical expressions
		Thermal conductivity
5.	Maïga et al.[41]	$\frac{\mu_{nf}}{\mu_f} = (1 + 7.3\phi + 123\phi^2)$
6.	Orozco[42]	$\frac{\mu_{nf}}{\mu_f} = (1 + 2.5\phi + 6.17\phi^2)$
7.	Nguyen et al.[43]	$\mu_{CuO} = -0.6967 + \frac{15.937}{T} + 1.238\phi + \frac{1556.14}{T^2} - 0.259\phi^2 - 30.88\frac{\phi}{T} - \frac{19652.74}{T^3} + 0.01593\phi^3 + 4.38206\frac{\phi^2}{T} + 147.573\frac{\phi}{T^2}$ $\mu_{Al_2O_3} = \exp(3.003 - 0.04203T - 0.5445\phi + 0.0002553T^2 + 0.0524\phi^2 - 1.622\phi^{-1})$
8.	Jang et al.[44]	$\frac{\mu_{nf}}{\mu_f} = (1 + 2.5\phi)\left[1 + \eta\left(\frac{d_p}{H}\right)^{-3\varepsilon}\phi^{2/3}(1+\varepsilon)\right]$
9.	Nguyen et al.[45]	$\frac{\mu_{nf}}{\mu_f} = (1 + 0.025\phi + 0.015\phi^2)$
10.	Gherasim et al.[46]	$\frac{\mu_{nf}}{\mu_f} = 0.904e^{14.8\phi}$
Electrical conductivity		
1.	Aminossadati et al.[47]	$\frac{\sigma_{nf}}{\sigma_f} = (1-\phi) + \phi\frac{\sigma_p}{\sigma_f}$
2.	Mahmoudi et al.[48]	$\frac{\sigma_{nf}}{\sigma_f} = 1 + \frac{3(\gamma-1)\phi}{(\gamma+2) - (\gamma-1)\phi}$ $\gamma = \frac{\sigma_p}{\sigma_f}$

Aminossadati et al.[47] have studied the magnetic field effect on forced convection of a nanofluid in a partially heated microchannel. They have considered the Al_2O_3 and water-based nanofluid and solved the problem using the finite volume based SIMPLE algorithm. They have examined the effect of various pertinent parameters and concluded that the microchannel performs better in terms of heat transfer at higher Reynolds and Hartmann numbers. For all Reynolds and Hartmann numbers, heat transfer enhances with increase in the nanoparticle volume fraction.

Chamkha and Aly[57] have studied the boundary layer flow of a nanofluid past a vertical flat plate. They have considered the Brownian motion and the thermophoresis effect. They have transformed the governing equations to a non-similar form and used numerical techniques to solve the same. They have reported that the local skin-friction coefficient increased as either of the suction, injection parameter, thermophoresis parameter, Lewis number, or heat generation or absorption parameter increased, while it decreased as either of the buoyancy ratio, Brownian motion parameter, or the magnetic field parameter increased.

Chamkha et al.[58] have studied the melting with heat generation and absorption effect of a nanofluid past a flat plate in the presence of a magnetic field. They have used the non-similar transformation and then numerically solved the governing equations. Based upon their numerical experiment, they have observed that the skin-friction coefficient increased as either of the Hartmann number or the melting parameter (Stefan number) increased. The Nusselt number was increased as either of the melting parameter, Brownian motion parameter, thermophoresis parameter, Lewis number or the heat generation coefficient was increased, whereas, it decreased as the strength of the magnetic field was increased.

Kandasamy et al.[59] have studied the MHD boundary layer flow of a nanofluid past a vertical stretching surface. They have considered the Brownian motion of the nanoparticles and used special Lie group transformation of the governing equations. They obtained the solution using the Runge-Kutta-Gill algorithm. They have concluded that the temperature of the fluid increases while the nanoparticle volume faction decreases with the increase in the Brownian motion and thermophorosis.

Ghasemi et al.[60] have studied the magneto-convection of Al_2O_3 nanofluid in an enclosure. He has taken the $\sigma_{nf}/\sigma_f = (1-\phi) + \phi\sigma_p/\sigma_f$ model to determine the effective electrical conductivity of a nanofluid and used the SIMPLE algorithm for numerical solution. Based upon the numerical experiment, they have concluded that the heat transfer rate increases with an increase in the Rayleigh

Table III. Summary of the numerical works on MHD flows and heat transfer of nanofluids.

Authors	Configurations	Nanoparticles and base fluid experimental/ numerical method	Studied parameters	Observations and conclusions
Aminossadati et al.[47]	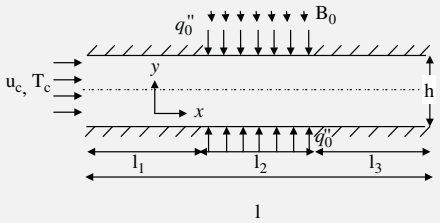	Forced convection of Al_2O_3 + water nanofluid flowing through a microchannel $\frac{\sigma_{nf}}{\sigma_f} = (1-\phi)+\phi\frac{\sigma_p}{\sigma_f}$ Finite volume based SIMPLE algorithm	Reynolds number, volume fraction and Hartmann number	Microchannel performs better in terms of heat transfer at higher Reynolds and Hartmann numbers. For all Reynolds and Hartmann numbers, heat transfer enhances with increase in volume fraction of nanoparticles.
Chamkha and Aly[57]	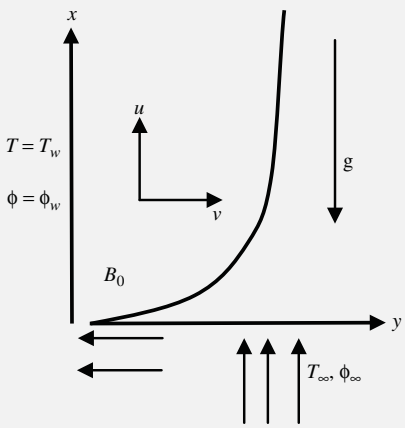	Brownian motion and thermophoresis Non-similar form transformation	Heat generation, absorption, suction and injection effects.	Local skin-friction coefficient increased as either of the suction or injection parameter, thermophoresis parameter, Lewis number, or the heat generation or absorption parameter increased, while it decreased as either the buoyancy ratio, Brownian motion parameter, or magnetic field parameter increased.
Chamkha et al.[58]	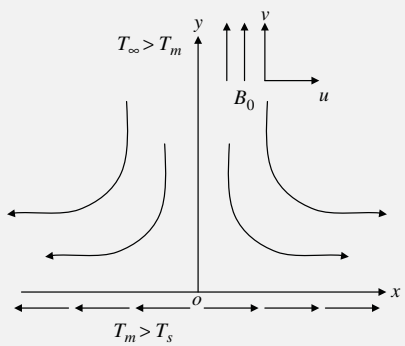	Melting and heat generation or absorption effects Non-Similar form transformation	Hartmann number, Stefan number	Skin-friction coefficient increased as either of the Hartmann number or the melting parameter (Stefan number) increased. The Nusselt number was increased as either of the melting parameter, Brownian motion parameter, thermophoresis parameter, Lewis number or the heat generation coefficient was increased, whereas, it decreased as the strength of the magnetic field was increased.
Kandasamy et al.[59]	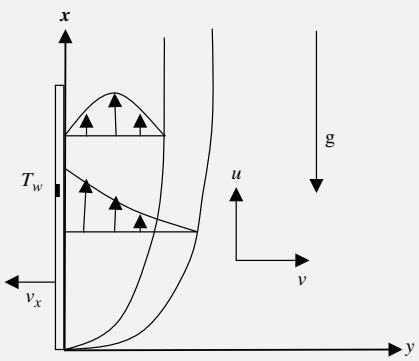	Analytical solution using special class of Lie group transformations Runge-Kutta-Gill algorithm	Lewis number, Magnetic field and Brownian parameters	Temperature of the fluid increases while the volume fraction of the nanoparticles decreases with the increase in Brownian motion and thermophoretic parameters

REVIEW

Table III. Continued.

Authors	Configurations	Nanoparticles and base fluid experimental/ numerical method	Studied parameters	Observations and conclusions
Ghasemi et al.[60]	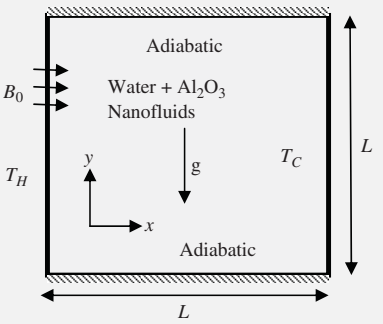	Al_2O_3 and water nanofluid $\frac{\sigma_{nf}}{\sigma_f} = (1-\phi) + \phi\frac{\sigma_p}{\sigma_f}$ SIMPLE algorithm	Rayleigh number, solid volume fraction, Hartmann number	Heat transfer rate increases with an increase in the Rayleigh number but it decreases with an increase in the Hartmann number. Increase of the solid volume fraction may result in enhancement or deterioration of the heat transfer performance depending on the values of Hartmann and Rayleigh numbers.
Hamad et al.[61]	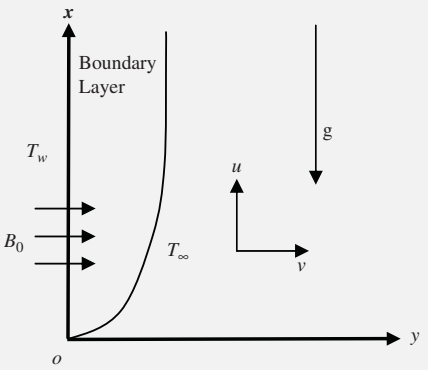	Cu, Ag, Al_2O_3 and water nanofluids. Conversion of PDEs to ODEs by similarity reduction technique	Magnetic parameters Flow volume fraction	Increasing the value of the magnetic parameter leads to a decrease of the velocity profiles and to an increase of the thermal profiles for fixed values of volume fraction. Cu and Ag nanoparticles proved to have the highest cooling performance for the problem considered.
Mahmoudi et al.[48]	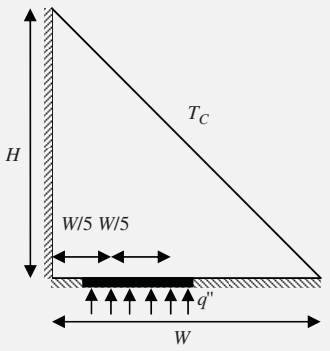	Triangular enclosure, partial heating below. Finite volume method	Hartmann number, Rayleigh number, volume fraction and active heating location	In presence of magnetic field, flow field is suppressed and heat transfer decreases. Furthermore, it is observed that maximum reduction of average Nusselt number at high value of Ha occurs at $Ra = 10^6$. It is found that nanoparticles are more effective at $Ra = 10^4$ where conduction is more pronounced.
Sheikholeslam et al.[62]	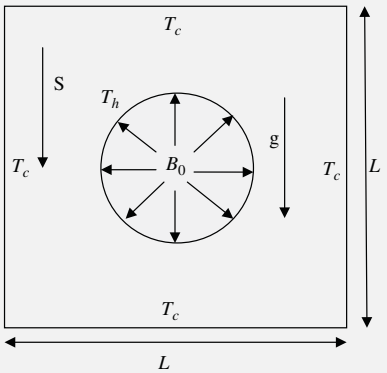	Lattice Boltzmann method Multi-distribution-function (MDF) model is used for simulating the effect of uniform magnetic field	Hartmann number, nanoparticles volume fraction and Rayleigh number	Average Nusselt number is an increasing function of nanoparticle volume fraction as well as the Rayleigh number, while it is a decreasing function of the Hartmann number

Table III. Continued.

Authors	Configurations	Nanoparticles and base fluid experimental/ numerical method	Studied parameters	Observations and conclusions
Sheikholeslam et al.[63]	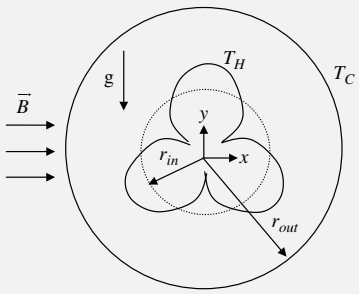	Cu-water nanofluid in a cold outer circular enclosure containing a hot inner sinusoidal circular cylinder in the presence of horizontal magnetic field. Control Volume based Finite Element Method (CVFEM)	Hartmann number, Rayleigh number, values of the number of undulations of the inner cylinder and nanoparticle volume fraction	In the absence of magnetic field, heat transfer enhancement ratio decreases as Rayleigh number increases while an opposite trend is observed in the presence of magnetic field. Average Nusselt number is an increasing function of nanoparticle volume fraction, the number of undulations and Rayleigh numbers while it is a decreasing function of Hartmann number.
Kefayati[64]	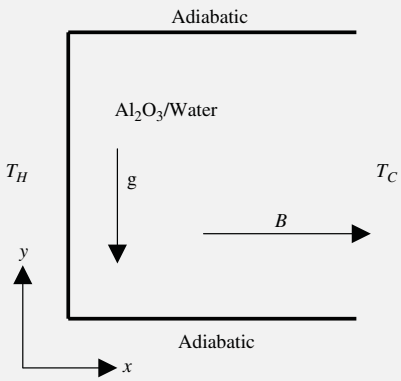	Al_2O_3-water nanofluid Lattice Boltzmann method	Rayleigh number, Hartmann number and nanoparticle volume fraction	Heat transfer decreases by the increment of Hartmann number for various Rayleigh numbers and volume fractions. The magnetic field augments the effect of nanoparticles at Rayleigh number of $Ra = 10^6$ regularly. For $Ra = 10^4$ and $Ha = 30$, nanoparticle effects are dominant. For $Ra = 10^5$ and $Ha = 60$, the presence of nanoparticles are more influential.
Kefayati[65]	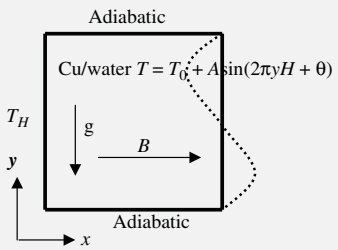	Cu and water-based nanofluid Lattice Boltzmann solution	Rayleigh number, Hartmann number, volume fraction of nanoparticles	At lower Rayleigh number, the growth of nanoparticles decreases the heat transfer in presence of magnetic field.
Mahmoudi et al.[66]	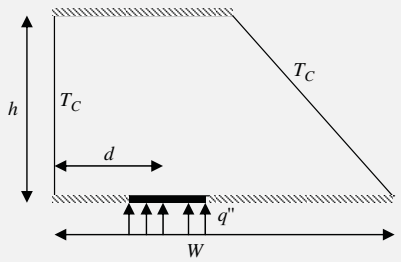	Cu +water Finite volume collocated method $\frac{\sigma_{nf}}{\sigma_f} = 1 + \frac{3(\gamma-1)\phi}{(\gamma+2)-(\gamma-1)\phi}$ $\gamma = \frac{\sigma_p}{\sigma_f}$	$Ra = 10^4 - 10^7$ $Ha = 0, 50, 100$ $\phi \leq 0.05$ $0 < \gamma < 180$	The entropy generation is decreased with the presence of the nanoparticles, while the same enhances with enhancement of magnetic field.

REVIEW

REVIEW

Table III. Continued.

Authors	Configurations	Nanoparticles and base fluid experimental/ numerical method	Studied parameters	Observations and conclusions
Ibrahim et al.[67]	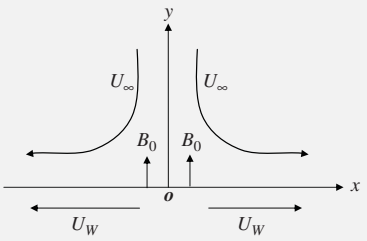	Fourth-order Runge-Kutta method	Velocity ratio parameter Prandtl number, Lewis number, Brownian motion, and the thermophoresis parameter	Skin friction coefficient, local Nusselt number and local Sherwood number are constant for unity velocity ratio.
Rashidi et al.[68]	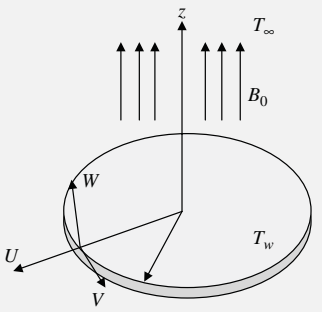	Cu, CuO, Al_2O_3+water Fourth-order Runge-Kutta method	Magnetic interaction parameter, suction parameter, nanoparticle volume fraction and the type of nanofluid	The fundamental objective of the second law thermodynamics analysis has been achieved by the minimization of entropy in the swirling disk flow regime, when the magnetic interaction parameter, suction parameter and nanoparticle volume fraction decreased.
Makinde et al.[69]	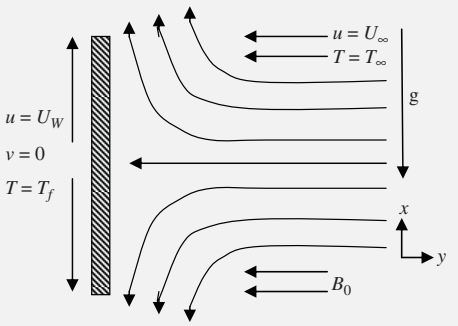	Fourth-order Runge-Kutta method	Buoyancy, convective heating, and magnetic parameters on the stagnation point flow and heat transfer	The dimensionless rescaled nanoparticle volume fraction decreases with increasing magnetic and stretching parameters.
Mahian et al.[70]	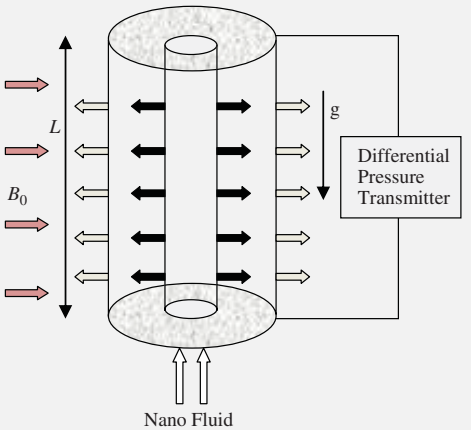	TiO_2+water Analytical solution using modified Bessel function of second kind	Pressure drop, Richardson number, Hartmann Number and nanoparticles concentrations	The entropy generation reduces with increases in TiO_2 nanoparticle concentration and enhances with increase in magnetic field.

Table III. Continued.

Authors	Configurations	Nanoparticles and base fluid experimental/ numerical method	Studied parameters	Observations and conclusions
Nandy and Mahapatra[71]	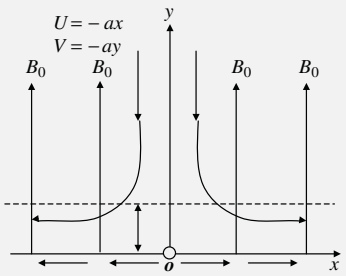	Similarity transformation, Shooting technique using Runge Kutta method	Brownian motion and thermo-phoresis, slip parameters, magnetic and source and sink parameters	Flow velocity, temperature and nanoparticle concentrations are strongly affected by slip parameters.
Jena and Mahapatra[72]	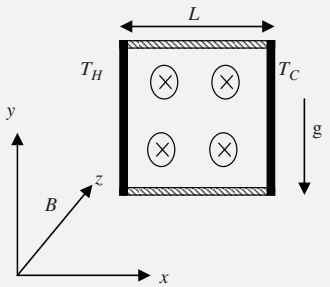	Atmospheric aerosol as nanofluid. Surface radiation Modified Mac method	Rayleigh number, Hartman number, volume fraction, radiation parameters	Surface radiation homogenizes the temperature distribution, equilibrates the core and enhances the heat transfer due to radiative heat flux. Its effect on heat transfer characteristics is independent of volume fraction and magnetic field
Sheikholeslami at al.[73]	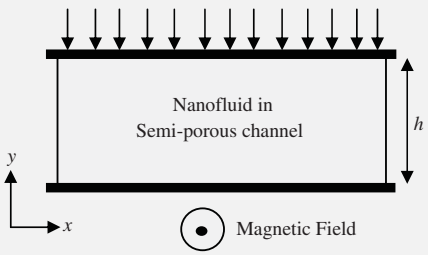	Least square Galerkin method Runge-Kutta method	Nanofluid Volume fraction, Hartmann number and Reynolds number.	The velocity boundary layer decreases with the increase in Reynolds number and the decrease in Hartmann number Cu and Ethylene-based nanofluid leads to maximum increment in velocity.
Sheikholeslami at al.[74]	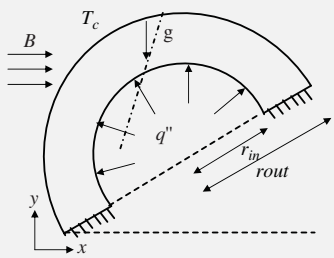	Cu-water nanoparticles Control Volume based Finite Element Method (CVFEM),	Hartmann number, Rayleigh number and inclination angle of enclosure	Hartmann number and the inclination angle of the enclosure are the controlling parameters at different Rayleigh numbers. In presence of magnetic field, velocity field retards and hence, convection and Nusselt number decrease.
Murthy et al.[75]	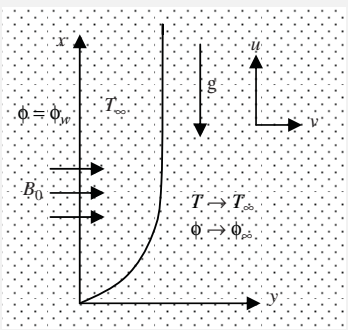	Non-Darcy porous medium under convective boundary condition. non-similar non-linear coupled partial differential equations	Nanoparticle volume fraction, Darcy number and Biot number	Thermal transportation is significantly affected due to the stratification of the medium. Heat transfer depends upon Biot number due to the convective boundary condition.

REVIEW

REVIEW

Table III. Continued.

Authors	Configurations	Nanoparticles and base fluid experimental/ numerical method	Studied parameters	Observations and conclusions
Mahmoudi et al.[76]	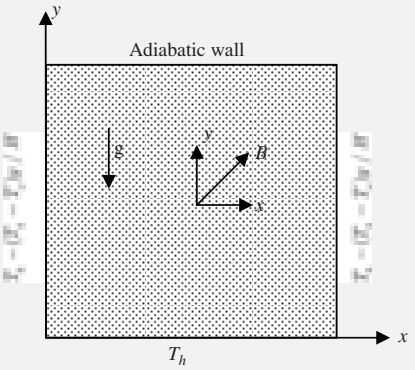	Lattice Boltzmann method Al_2O_3 + water	$Ra = 10^3 - 10^5$ $Ha = 0 - 60$ $\phi = 0 - 0.06$ $0 < \gamma < 180$	The magnetic field direction controls the effect of nanoparticles in the fluid. For high Hartmann number (Ha = 30), the most intense effect of nanoparticles is for $\gamma = 0°$, the effect of nanoparticles is negative for $\gamma = 60°$ to 120°.
Mejri et al.[77]	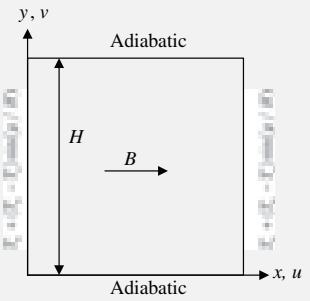	Al_2O_3 and water nanofluids, Lattice Boltzmann method	Rayleigh number, Hartmann number, phase deviation and solid volume fraction	For $Ra = 5 \times 10^4$ and Ha = 20, the heat transfer rate and entropy generation respectively increase and decrease with the increases of volume fraction. For Ha = 50 and $\gamma = \frac{\pi}{2}$, adding nanoparticles increases heat transfer rate but does not affect the entropy generation.
Sheikholeslami et al.[49]	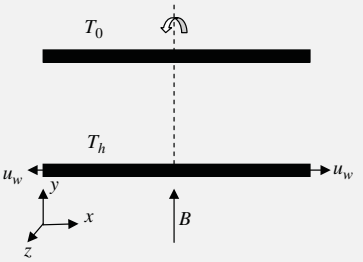	$\frac{\sigma_{nf}}{\sigma_f} = 1 + \frac{3(\gamma-1)\phi}{(\gamma+2)-(\gamma-1)\phi}$ $\gamma = \frac{\sigma_p}{\sigma_f}$ Runge-Kutta method	Brownian motion, magnetic parameter, rotation parameters and Reynolds number	Nusselt number is enhanced with increases in Reynolds and nanoparticle volume fraction, while it decreases with increases in Eckert and magnetic and rotation parameters.
Sheikholeslami and Ganji[78]	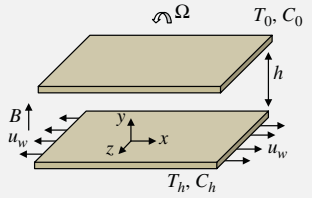	Runge-Kutta method	Brownian motion, thermophorosis, Reynolds number, rotation parameters and magnetic parameters	Nusselt number has a direct relationship with Reynolds number and inverse relationship with rotation, magnetic, thermophoretic and Brownian parameters and Schimidt number.
Sheikholeslami et al.[79]	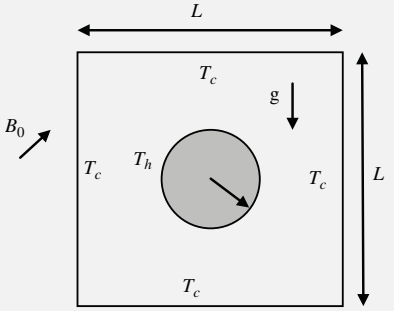	Cu + water nanofluid. Lattice Boltzmann method	Nanoparticle volume fraction, Hartmann number, aspect ratio and Rayleigh number	Heat transfer enhancement ratio increases with decrease in Rayleigh number and increases with increase in Hartmann number.

Table III. Continued.

Authors	Configurations	Nanoparticles and base fluid experimental/ numerical method	Studied parameters	Observations and conclusions
Sheikholeslami et al.[80]	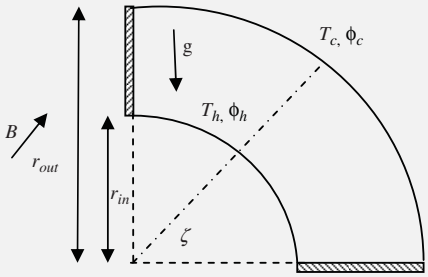	Al_2O_3 + water nanofluids Finite element method Heatline visualization	Hartmann number, Buoyancy ratio, Lewis number	The results indicate that Nusselt number is an increasing function of buoyancy ratio number but it is a decreasing function of Lewis number and Hartmann number.
Sheikholeslami et al.[81]	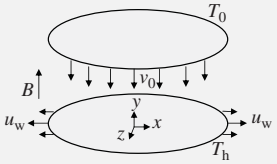	Cu, Ag, Al_2O_3, TiO_3 and water nanofluids. Runge-Kutta method	Nanofluid volume fraction, magnetic parameter, wall injection/suction parameter, viscosity parameter and rotation parameter	The results indicate that, for both suction and injection the Nusselt number has a direct relationship with the nanoparticle volume fraction. The highest values are obtained when titanium oxide is used as a nanoparticle.
Sheikholeslami et al.[82]	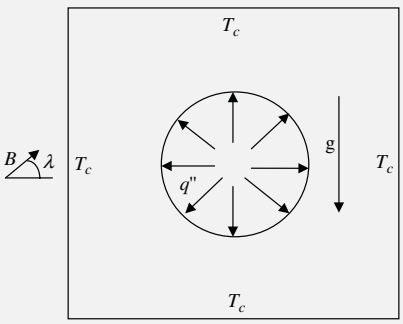	KKL (Koo-Kleinstreuer-Li) correlation is used for simulating effective thermal conductivity and viscosity of nanofluid. Finite Element Method	Hartmann number, volume fraction of nanoparticle, Rayleigh number and aspect ratio	The results show that as Hartmann number increases, Nusselt number decreases while opposite trend is observed as nanoparticles volume fraction, Rayleigh number and aspect ratio increase.
Sheikholeslami et al.[83]	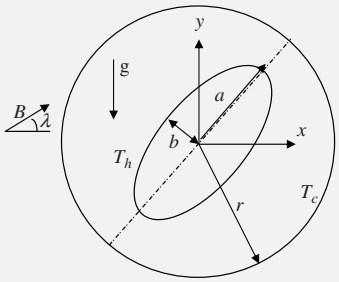	Cu-water nanofluid, Control Volume based Finite Element Method (CVFEM),	Hartmann number, Rayleigh number, nanoparticle volume fraction and inclined angle of inner cylinder.	Nusselt number is an increasing function of nanoparticle volume fraction, Rayleigh number, inclination angle and a decreasing function of Hartmann number. Effect of inclination angle on Nusselt number becomes smaller in presence of magnetic field.
Sheikholeslami et al.[84]	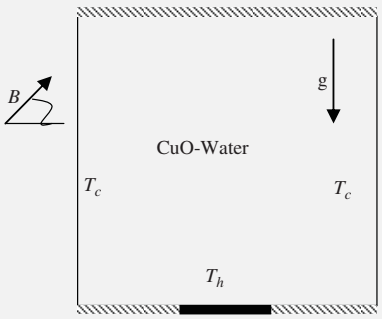	Cu-Water nanofluid Lattice Boltzmann method KKL(Koo–Kleinstreuer–Li) correlation	Hartmann number, heat source length, nanoparticle volume fraction and Rayleigh numbers	The enhancement in heat transfer increases as Hartmann number and heat source length increase but it decreases with increase of Rayleigh number. The effect of Hartmann number and heat source length is more pronounced at high Rayleigh number.

REVIEW

Table III. Continued.

Authors	Configurations	Nanoparticles and base fluid experimental/ numerical method	Studied parameters	Observations and conclusions
Sheikholeslami et al.[85]	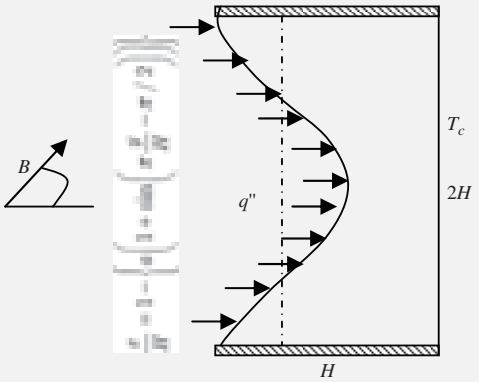	CuO–water nanofluid, Control volume based finite element method (CVFEM), KKL (Koo–Kleinstreuer–Li) correlation	Volume fraction of nanoparticles, Rayleigh number, dimensionless amplitude of the sinusoidal wall, Hartmann number	Nusselt number is an increasing function of nanoparticles volume fraction, dimensionless amplitude of the sinusoidal wall and Rayleigh number while it is a decreasing function of Hartmann number.
Chamkha and Rashad[86]	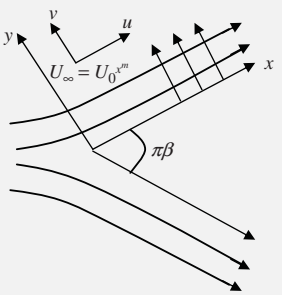	Boundary layer flow around a non-isothermal wedge Brownian motion and Thermophoresis Finite difference method	Magnetic parameter, Pressure gradient parameter	Local skin-friction coefficient, local Nusselt number, and the local Sherwood number reduced as either of the magnetic parameter or the pressure gradient parameter is increased. The presence of the Brownian motion and the thermophoresis effects caused the local Nusselt number to decrease and the Sherwood number to increase.
Chamkha et al.[87]	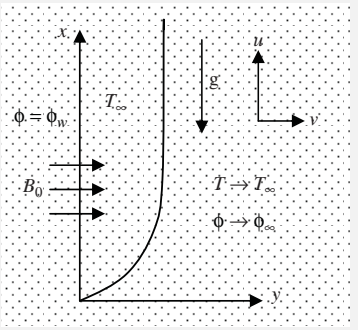	Viscous dissipation and magnetic field effects on nanofluid flow in non-Darcy porous medium. Implicit finite difference method	Magnetic field, viscous dissipation and non-Darcy medium	The presence of MHD and viscous dissipation effects in the nanofluid saturated non-Darcy porous medium influenced the flow, heat, and the nanoparticle volume fraction significantly.
Mehrez et al.[88]	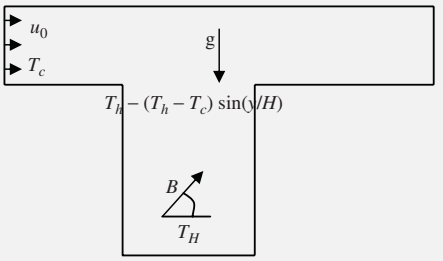	Cu-water nanofluid flow in an open cavity heated from below. finite-volume method, $\frac{\sigma_{nf}}{\sigma_f} = (1-\phi) + \phi\frac{\sigma_p}{\sigma_f}$	Solid volume fraction Hartmann number Reynolds number Richardson number inclination angles of magnetic field	Average Nusselt number and entropy generation increase by increasing volume fraction of nanoparticles and this depends mainly on the Hartmann number and inclination angle of the magnetic field. The variation rates of heat transfer and entropy generation while adding nanoparticles or applying a magnetic field depend on the Richardson and Reynolds numbers.

Table III. Continued.

Authors	Configurations	Nanoparticles and base fluid experimental/ numerical method	Studied parameters	Observations and conclusions
Sheikholeslami et al.[89]	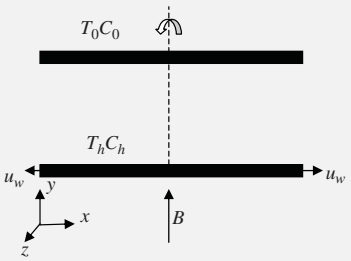	Thermal radiation, Brownian motion and thermophores Fourth-order Runge-Kutta method	Reynolds number, magnetic parameter, rotation parameter, Schmidt number, thermophoretic parameter, Brownian parameter and radiation parameter	Nusselt number has direct relationship with radiation parameter and Reynolds number while it has reverse relationship with other active parameters. Concentration boundary layer thickness decreases with the increase of radiation parameter.
Sheikholeslami et al.[90]	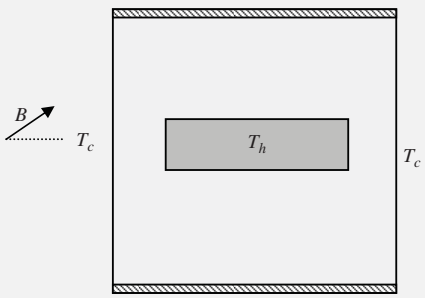	CuO–water nanofluid, Lattice Boltzmann Method (LBM) KKL (Koo–Kleinstreuer–Li) correlation	Hartmann number, nanoparticle volume fraction and Rayleigh number on the flow	Heat transfer rate and dimensionless entropy generation number increase with increase of the Rayleigh number and nanoparticle volume fraction but it decreases with increase of the Hartmann number.
Gireesha et al.[91]	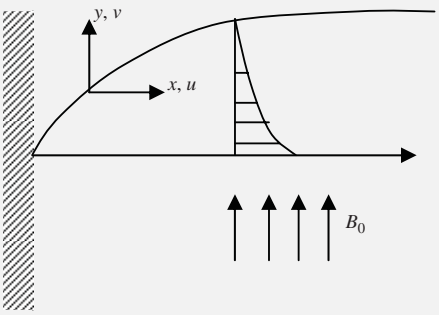	Nanofluid with homogeneously suspended dust particles. Similarity transformation and Runge-Kutta-Fehlberg fourth-fifth order method for numerical solution	Nanoparticle volume fraction, magnetic parameter, fluid particle interaction parameter, Prandtl number, Eckert number	Temperatures of nanofluid and dust phase increase with increasing values of Eckert number. Velocities of nanofluid and dust phase decrease while temperatures of nanofluid and dust phase increase as solid volume fraction of nanoparticle increases. It is found that the dusty fluid with copper nanoparticles has an appreciable cooling performance.

number but it decreases with an increase in the Hartmann number. Increasing the solid volume fraction may result in enhancement or deterioration of the heat transfer performance depending on the value of the Hartmann and Rayleigh numbers.

Hamad et al.[61] have studied the convection of a nanofluid past a semi-infinite vertical flat plate. They have considered Cu, Ag, Al_2O_3 and water-based nanofluids and used the similarity reduction techniques to convert the PDEs into ODEs. Then, they have numerically solved the ODEs. Based upon the numerical observation, they have reported that, increasing the values of the magnetic parameter leads to a decrease in the velocity profiles and to an increase in the thermal profiles for fixed values of the particles volume fraction. Cu and Ag nanoparticles proved to have the highest cooling performance for the problem considered.

Mahmoudi et al.[48] have studied the magneto-convection in a triangular enclosure for six different heating conditions. In their numerical observation, they have concluded that, in the presence of a magnetic field, the flow field is suppressed and heat transfer decreases. Furthermore, they reported that the maximum reduction of the average Nusselt number at high value of Ha occurs at $Ra = 10^6$. It is found that the nanoparticles are more effective at $Ra = 10^4$, where conduction is more pronounced.

Sheikholeslam et al.[62] have studied the MHD flow of nanofluids in an annulus. They have considered the Multi-Distribution-Function (MDF) model for simulating the effect of uniform magnetic field and the lattice Boltzmann

REVIEW

method for numerical solution. They have reported that the average Nusselt number is an increasing function of the nanoparticle volume fraction as well as the Rayleigh number, while it is a decreasing function of the Hartmann number.

Sheikholeslam et al.[63] have studied convection of Cu-water nanofluid in a cold outer circular enclosure containing a hot inner sinusoidal circular cylinder in the presence of a horizontal magnetic field. They have used the Control Volume based Finite Element Method (CVFEM) for the numerical solution and reported that, in the absence of magnetic field, the heat transfer enhancement ratio decreases as the Rayleigh number increases while an opposite trend is observed in the presence of a magnetic field. The average Nusselt number is an increasing function of the nanoparticle volume fraction, the number of undulations and the Rayleigh numbers while it is a decreasing function of the Hartmann number.

Kefayati[64] have studied the magneto-convection of Al_2O_3 water-based nanofluid in an open enclosure using the Lattice Boltzmann method. They have reported that heat transfer decreases by the increment of the Hartmann number for various Rayleigh numbers and volume fractions. The magnetic field augments the effect of the nanoparticles at a Rayleigh number of $Ra = 10^6$ regularly. For $Ra = 10^4$ and $Ha = 30$, nanoparticle effects are dominant. For $Ra = 10^5$ and $Ha = 60$, the presence of nanoparticles are more influential.

Kefayati[65] has analyzed the heat transfer from a cavity filled with Cu and water-based nanofluids with a sinusoidal temperature distribution. He has used the lattice Boltzmann method for the numerical solution. He has reported that in the presence of a magnetic field, the heat transfer decreases with the increase in the nanoparticle volume fraction at low Rayleigh numbers.

Mahmoudi et al.[66] have done the finite volume based numerical solution of Cu and water-based nanofluid in a trapezoidal cavity in the presence of a magnetic field. They have observed minimization of entropy generation with an increase in the nanoparticle concentration and that the magnetic field enhances the entropy of the system considered.

Ibrahim et al.[67] have done the simulation for heat transfer due to a nanofluid towards the stagnation point of a stretching sheet with MHD effects. They have used the fourth-order Runge-Kutta method for the solution. They have reported that the values of the Nusselt number, Sherwood number and the skin friction become constant when the velocity ratio parameter reaches unity.

Rashidi et al.[68] have considered the entropy generation during the rotation of a porous disk in a nanofluid in the presence of a magnetic field. Their study is intended for MHD-based rotating energy generator used in nuclear propulsion space vehicles. They have used Cu, CuO and Al_2O_3 and water nanofluids in their study. They have reduced the governing equations to the form of ordinary differential equations and used the Runge-Kutta method for the solution. They have reported minimization of entropy in the swirling disk flow regime when the magnetic interaction, suction parameter and nanoparticle volume fraction decreased.

Makinde et al.[69] have studied the buoyancy effect on MHD flow of a nanofluid around a stretching and shrinking sheet. They have used the Runge-Kutta method to solve the MHD stagnation-point flow considering the buoyancy, convective heating and magnetic parameters. They have noticed the decrease in dimensionless rescaled nanoparticle volume fraction with the increase in the magnetic and stretching parameters.

Mahian et al.[70] have studied the irreversibility on the MHD flow of TiO_3 nanofluid in a vertical annulus. They have derived an analytical solution using the modified Bessel number of the second kind. They have considered the effect of nanoparticle, volume fraction, pressure drop, Richardson number and the Hartmann number on the flow and concluded that the entropy minimizes with increases in the TiO_2 concentration and increases with the increase in the Hartmann number.

Nandy and Mahapatra[71] have studied the effect of slip for MHD stagnation flow near the stretching and shrinking sheet using nanofluids. They have used the similarity transformation relation to bring the governing partial differential equations into ordinary differential equations. Then, they solved the governing ODEs with the shooting method employing the Runge-Kutta scheme. They have reported the influence of slip velocity on temperature, velocity and nanoparticle concentrations.

Jena and Mahapatra[72] have studied the magneto-convection of atmospheric aerosol regarded as nanofluids. They have examined the surface radiation effects on the phenomenon and reported that the surface radiation homogenizes the temperature distribution, equilibrates the core and enhances the heat transfer due to radiative heat flux. They have found that its effect on heat transfer characteristics is independent of the volume fraction and the magnetic field.

Sheikholeslami et al.[73] have studied the MHD flow of nanofluid in a semi-porous channel. They have used both the Runge-Kutta and Least square-based Galerkin method for the numerical solution. They have considered the nanoparticle volume fraction, Reynolds number and the Hartmann number variation. They have reported that the velocity boundary layer decreases with the increase in the Reynolds number and the decrease in the Hartmann number. They have also concluded that Cu and Ethylene-based nanofluid leads to maximum increment in that velocity.

Sheikholeslami et al.[74] studied the magneto-convection of Cu and water-based nanofluid in a curved geometry using the Control Volume based Finite Element Method (CVFEM). From their study, they have reported that the

Hartmann number and the inclination angle of the enclosure are the controlling parameters at different Rayleigh numbers. In the presence of a magnetic field, the velocity field retarded and hence, the convection and the Nusselt number decrease.

Murthy et al.[75] have studied the convection of a nanofluid in a non-Darcy porous medium with convective boundary conditions. They have solved the non-similar nonlinear partial differential equations numerically. From their observation, they have concluded that the thermal transportation is significantly affected due to the stratification of the medium and that heat transfer depended upon the Biot number due to the convective boundary condition.

Mahmoudi et al.[76] have studied the MHD natural convection in a cavity with a linear temperature distribution. They have used the Lattice Boltzmann method for the numerical solution of Al_2O_3 and water-based nanofluids. They have concluded that the magnetic field direction controls the effect of the nanoparticles in the fluid. They have reported that for a high Hartmann number ($Ha = 30$), the most intense effect of nanoparticles is for the inclination angle of the magnetic field $\gamma = 0^0$ while the effect of nanoparticles is negative for $\gamma = 60°$ to $\gamma = 120°$.

Mejri et al.[77] have studied the natural convection heat transfer and entropy generation in a cavity filled with a nanofluid in the presence of a magnetic field and a sinusoidal temperature distribution. They have used the lattice Boltzmann method for the solution of Al_2O_3 and water nanofluids. They have reported that, for $Ra = 5 \times 10^4$ and $Ha = 20$, the heat transfer rate and entropy generation respectively increase and decrease with the increases of the volume fraction. However, for $Ha = 50$ and $\gamma = \pi/2$, adding nanoparticles increases the heat transfer rate but does not affect the entropy generation.

Sheikholeslami et al.[49] have considered the viscous dissipation effect of MHD nanofluid flow. They have considered the Brownian motion of nanoparticles and used the Koo-Kleinstreuer-Li correlations. The governing equations are solved using the Runge Kutta method. They have reported enhancement of the Nusselt number with the increase in the Reynolds number and the nanoparticle volume fraction, while they have noticed decreases in the Nusselt number with increases in the Eckert number and the magnetic and rotation parameters.

Sheikholeslami and Ganji[78] have studied heat and mass transfer from a rotating system of a nanofluid in the presence of a magnetic field. They have used the Runge-Kutta method for the solution. After a detailed parametric study, they concluded that the Nusselt number has a direct relationship with the Reynolds number and an inverse relationship with the rotation, magnetic, thermophoretic and the Brownian parameters as well as the Schimidt number.

Sheikholeslami et al.[79] have considered the natural convection of a nanofluid inside a square cavity having a concentric cylindrical annulus. They have used the Lattice Boltzmann method for the numerical solution. They have observed the increase in the heat transfer enhancement ratio with the increase in the Hartmann number and the decrease in the Rayleigh number.

Sheikholeslami et al.[80] have studied free convection of an Al_2O_3–water nanofluid in curved structure geometry. They have used the finite element method for the numerical solution. They have also done heatline visualization of the phenomenon. They have reported that, the Nusselt number is an increasing function of the buoyancy ratio number but it is a decreasing function of the Lewis number and the Hartmann number.

Sheikholeslami et al.[81] have considered MHD convection of nanofluids in a rotating system. They have used Cu, Ag, Al_2O_3, TiO_3 and water nanofluids and adopted the Runge-Kutta method for the numerical solution. After a detailed parametric study, they have concluded that for both suction and injection, the Nusselt number has a direct relationship with the nanoparticle volume fraction. The highest values are obtained when titanium oxide is used as the nanoparticle type.

Sheikholeslami et al.[82] have studied the MHD free convection of nanofluids in a concentric annulus. They have used the KKL (Koo-Kleinstreuer-Li) correlation for simulating the effective thermal conductivity and viscosity of the nanofluid. They used the Finite Element Method (FEM) for the numerical simulation. They have reported that as the Hartmann number increases, the Nusselt number decreases while the opposite trend is observed as the nanoparticles volume fraction, Rayleigh number and the aspect ratio increase.

Sheikholeslami et al.[83] have studied the natural convection of Cu and water-based nanofluid in an enclosure with a hot elliptic cylinder placed at the center in the presence of a magnetic field. They have used the Control Volume based Finite Element Method (CVFEM) for solution. They observed and concluded that the Nusselt number is an increasing function of the nanoparticle volume fraction, Rayleigh number, and the inclination angle and a decreasing function of the Hartmann number. The effect of the inclination angle on the Nusselt number becomes smaller in the presence of the magnetic field.

Sheikholeslami et al.[84] have studied the natural convection of CuO and water nanofluid in a rectangular enclosure in the presence of a magnetic field considering the Lorentz force effect. They have considered the Koo–Kleinstreuer–Li relationship for evaluating the nanofluid properties which accounts for the Brownian motion of nanoparticles. They have used the lattice Boltzmann method for the numerical simulation. They have reported that the enhancement in heat transfer increases as the Hartmann number and the heat source length increase but it decreases with the increase in the Rayleigh number. Further, they mentioned that the effects of the Hartmann number and the heat source length are more pronounced at high Rayleigh numbers.

Sheikholeslami et al.[85] have examined the heat transfer characteristics from a sinusoidal wall filled with a nanofluid in the presence of a magnetic field. They have used the KKL (Koo–Kleinstreuer–Li) correlation to calculate the properties of CuO nanofluid and obtained the solution using the Control Volume based Finite Element Method (CVFEM). Based upon the numerical calculations, they have reported that the Nusselt number is an increasing function of the nanoparticles volume fraction, dimensionless amplitude of the sinusoidal wall and the Rayleigh number while it is a decreasing function of the Hartmann number.

Chamkha and Rashad[86] have studied the flow of a nanofluid around a non-isothermal wedge. They have considered the Brownian movement and the thermophoresis effects. They have concluded that the local skin-friction coefficient, local Nusselt number, and the local Sherwood number reduced as either of the magnetic parameter or the pressure gradient parameter was increased. The presence of the Brownian motion and the thermophoresis effects caused the local Nusselt number to decrease and the Sherwood number to increase.

Chamkha et al.[87] have studied the effects of viscous dissipation and magnetic field on natural convection of a nanofluid past a vertical plate in a saturated non-Darcy porous medium. From their finite difference numerical solution, they have concluded that the presence of MHD and viscous dissipation effects in the nanofluid-saturated non-Darcy porous medium influenced the flow, heat, and the nanoparticle volume fraction significantly.

Mehrez et al.[88] have studied the natural convection of Cu-water nanofluid flow in an open cavity heated from below. They have considered the electrical conductivity of a nanofluid by the relation $\frac{\sigma_{nf}}{\sigma_f} = (1-\phi) + \phi\sigma_p/\sigma_f$. They have used the finite volume method for the numerical solution. In their findings, they have reported that the average Nusselt number and the entropy generation increase by increasing the volume fraction of nanoparticles, and this depends mainly on the Hartmann number and inclination angle of the magnetic field. They have concluded that the variation rates of heat transfer and the entropy generation while adding nanoparticles or applying a magnetic field depend on the Richardson and Reynolds numbers.

Sheikholeslami et al.[89] have studied the effect of thermal radiation on magnetohydrodynamic nanofluid flow between two horizontal rotating plates. They have reduced the nonlinear PDEs to coupled ODEs and then solved the same using the fourth-order Runge-Kutta method. Based upon their observation, they have reported that the Nusselt number has a direct relationship with the radiation parameter and the Reynolds number while it has the reverse relationship with the other active parameters and that the concentration boundary layer thickness decreases with the increase in the radiation parameter.

Sheikholeslami et al.[90] have studied the entropy generation of nanofluids in the presence of a magnetic field. They have considered the KKL (Koo–Kleinstreuer–Li) correlation to determine the properties of the Cu water-based nanofluid and adopted the lattice Boltzmann method for the numerical solution. They have reported that the heat transfer rate and the dimensionless entropy generation number increase with the increase of the Rayleigh number and the nanoparticle volume fraction but it decreases with the increase of the Hartmann number.

Recently, Gireesha et al.[91] have studied the MHD boundary layer flow and heat transfer of an incompressible nanofluid with homogeneously suspended dust particles. The flow is generated due to a linear stretching surface in the presence of uniform magnetic field. They performed the similarity transformation and used the Runge-Kutta-Fehlberg fourth-fifth order method for the numerical solution. Based upon their numerical observation, they concluded that the temperatures of the nanofluid and the dust phase increase with increasing values of the Eckert number. In addition, they reported that the velocities of the nanofluid and the dust phase decrease while the temperatures of the nanofluid and the dust phase increase as the solid volume fraction of nanoparticles increases. They concluded that the dusty fluid with copper nanoparticles has an appreciable cooling performance.

3. CONCLUSION

Nanofluids are a new class of smart fluids that are of paramount importance in numerous applications involving heat transfer. Many important reviews have been reported in the literature on the studies done on nanofluids in the past decade or so. These studies highlight interesting physical phenomena regarding heat transfer enhancement, cooling and control involving the use of nanofluids. Much attention has been given to the measurement and the development of models for the nanofluid's thermal conductivity, viscosity and other properties and their effects on the heat transfer characteristics. In the past decade, a lot of work has been done on MHD convective flow of nanofluids, but the review of these types of flow and heat transfer situations is absent from the literature till date. This paper reports an overview of the recent developments in the study of MHD convection heat transfer using nanofluids in various geometries and applications. Much work still needs to be done in the area of nanofluids, specifically on the problems of nanoparticles agglomeration, settling, and erosion, particle size and shape distribution, clustering, etc. and their potential effects in the applications. Also, more research needs to be performed on the true understanding of the physical mechanisms at the nanoscale level due to the lack of agreement in some cases between experimental measurements and theoretical studies dealing with nanofluids. Accurate nanofluids properties models based on accurate experimental work are still needed and many other factors still need to be explored and optimized and more promising potential applications need to be identified.

NOMENCLATURE

C_p Specific heat at constant pressure
d Diameter
g Gravitational acceleration
k Thermal conductivity
p Pressure
Pr Prandtl number
Pe Peclet number
Re Reynolds number
T Temperature
V Nanofluid velocity.

Greek Symbols

μ Dynamic viscosity
τ Stress tensor
ϕ Nanoparticle volume fraction
ρ Density
σ Electrical conductivity.

Subscripts

f Base fluid
eff Effective
nf Nanofluid
p Particle.

References and Notes

1. W. Oswald, The World of Neglected Dimensions, Dresden, Germany (**1915**).
2. J. C. Maxwell, A Treatise on Electricity and Magnetism, 2nd edn., Clarendon Press, Oxford, UK (**1881**).
3. C. G. Granquist and R. A. Buhrman, *J. Appl. Phys.* 47, 2200 (**1976**).
4. S. U. S. Choi, Enhancing thermal conductivity of fluids with nanoparticles, Developments and Applications of Non-Newtonian Flows (**1995**), FED-Vol. 231/MD-Vol. 66, pp. 99–105.
5. S. U. S. Choi, *ASME Fluids Engineering Division* 231, 99 (**1995**).
6. J. A. Eastman, S. U. S. Choi, S. Li, L. J. Thompson, and S. Lee, Enhancement thermal conductivity through the development of nanofluids, 1996 Fall meeting of the Materials Research Society (MRS), Boston, USA (**1997**).
7. P. Keblinski, J. A. Eastman, and D. G. Cahill, *Mater. Today* 8, 36 (**2005**).
8. W. Xiang-Qi and A. S. Mujumdar, *Int. J. Thermal Sciences* 46, 1 (**2007**).
9. S. K. Das, S. U. S. Choi, and H. E. Patel, *Heat Transfer Engineering* 27, 3 (**2006**).
10. V. Trisaksri and S. Wongwises, *Renewable and Sustainable Energy Reviews* 11, 512 (**2007**).
11. H. Masuda, A. Ebata, K. Teramae, and N. Hishinuma, *Netsu Bussei* 7, 227 (**1993**).
12. S. Lee, S. U. S. Choi, S. Li, and J. A. Eastman, *Trans. ASME, J. Heat Transfer* 121, 280 (**1999**).
13. Y. Xuan and Q. Li, *Int. J. Heat Fluid Flow* 21, 58 (**2000**).
14. Y. Xuan and W. Roetzel, *Int. J. Heat Mass Transfer* 43, 3701 (**2000**).
15. S. U. S. Choi, Z. G. Zhang, W. Yu, F. E. Lockwood, and E. A. Grulke, *Appl. Phys. Lett.* 79, 2252 (**2001**).
16. S. Mirmasoumi and A. Behzadmehr, *Appl. Therm. Eng.* 28, 717 (**2008**).
17. V. Bianco, O. Manca, and S. Nardini, *International Journal of Thermal Sciences* 29, 3632 (**2009**).
18. A. Akbarinia and R. Laur, *Int. J. Heat Fluid Flow* 30, 706 (**2009**).
19. E. Abu-Nada and H. F. Oztop, *Int. J. Heat Fluid Flow* 30, 669 (**2009**).
20. E. Abu-Nada, *Int. J. Heat Fluid Flow* 30, 679 (**2009**).
21. O. Abouali and A. Falahatpisheh, *Journal of Heat and Mass Transfer* 46, 15 (**2009**).
22. B. C. Pak and Y. I. Cho, *Exp. Heat Transfer* 11, 151 (**1998**).
23. S. E. B Maïga, C. T. Nguyen, N. Galanis, and G. Roy, *Superlattices Microstructures* 35, 543 (**2004**).
24. S. J. Palm, G. Roy, and C. T. Nguyen, *Appl. Therm. Eng.* 26, 2209 (**2006**).
25. J. A. Eastman, S. U. S. Choi, S. Li, G. Soyez, L. J Thompson, and R. J. Di Melfi, *Material Science Forum* 3, 312 (**1999**).
26. S. K. Das, S. U. S Choi, W. Yu, and T. Pradeep, Nanofluids Science and Technology, John Wiley and Sons, Hoboken, NJ (**2008**).
27. D. A. G. Bruggeman, *Annalen der Physik, Leipzig* 24, 636 (**1935**).
28. R. L. Hamilton and O. K. Crosser, *Ind. Eng. Chem. Fundam.* 1, 182 (**1962**).
29. D. J. Jeffrey, *Proceedings of Royal Society A* 335, 355 (**1973**).
30. R. H. Davis, *International Journal of Thermo Physics* 7, 609 (**1986**).
31. S. Lu and H. Lin, *J. Appl. Phys.* 79, 6761 (**1996**).
32. W. Yu and S. U. S. Choi, *J. Nanoparticle Res.* 5, 167 (**2003**).
33. H. E. Patel, T. Sundarrajan, T. Pradeep, A. Dasgupta, N. Dasgupta, and S. K. Das, *Pramana Journal of Physics* 65, 863 (**2005**).
34. H. A. Mintsa, G. Roy, C. T. Nguyen, and D. Doucet, *International Journal of Thermal Science* 48, 363 (**2009**).
35. J. Koo and C. Kleinstreuer, *Journal of Nanoparticle Research* 6, 577 (**2004**).
36. R. Prasher, *Journal of Heat Transfer* 128, 588 (**2006**).
37. S. P. Jang and S. U. S. Choi, *ASME J Heat Transfer* 129, 617 (**2007**).
38. J. Li, Computational analysis of nanofluid flow in microchannels with applications to micro-heat sinks and bio-MEMS, PhD Thesis NC State University, Raleigh, NC, the United States (**2008**).
39. H. C. Brinkman, *The Journal of Chemical Physics* 20, 571 (**1952**).
40. A. Einstein, Investigation on the Theory of Brownian Motion, Dover, New York (**1956**).
41. S. E. B Maïga, S. M. Palm, C. T. Nguyen, G. Roy, and N. Galanis, *Int. J. Heat Fluid Flow* 26, 530 (**2005**).
42. D. Orozco, *Encyclopedia Surface Colloid Science* 4, 2375 (**2005**).
43. C. T. Nguyen, F. Desgranges, G. Roy, N. Galanis, T. Mare, S. Boucher, and H. A. Minsta, *Int. J. Heat Fluid Flow* 28, 1492 (**2007**).
44. S. P. Jang, J. H. Lee, K. S. Hwang, and S. U. S. Choi, *Appl. Phys. Lett.* 91, 243112 (**2007**).
45. C. T. Nguyen, F. Desgranges, N. Galanis, G. Roy, T. Mare, S. Boucher, and H. A. Mintsa, *International Journal of Thermal Science* 47, 103 (**2008**).
46. I. Gherasim, G. Roy, C. T. Nguyen, and D. Vo-Ngoc, *International Journal of Thermal Science* 48, 1486 (**2009**).
47. S. M. Aminossadati, A. Raisi, and B. Ghasemi, *International Journal of Non-Linear Mechanics* 46, 1373 (**2011**).
48. A. H. Mahmoudi, I. Pop, and M. Shahi, *International Journal of Thermal Sciences* 59, 126 (**2012**).
49. M. Sheikholeslami, S. Abelman, and D. D. Ganji, *Int. J. Heat Mass Transfer* 79, 212 (**2014**).
50. S. Kakaç and A. Pramuanjaroenkij, *Int. J. Heat Mass Transfer* 52, 3187 (**2009**).
51. G. Paul, M. Chopkar, I. Manna, and P. K. Das, *Renewable and Sustainable Energy Reviews* 14, 1913 (**2010**).
52. C. Kleinstreuer and F. Yu, *Nanoscale Research Letters* 6, 1 (**2011**).
53. M. Corcione, *Energy Conversion and Management* 52, 789 (**2011**).
54. A. Ghadimi, R. Saidur, and H. S. C. Metselaar, *Int. J. Heat Mass Transfer* 54, 4051 (**2011**).
55. Z. Haddad, H. F. Oztop, E. Abu-Nada, and A. Mataoui, *Renewable and Sustainable Energy Reviews* 16, 5363 (**2012**).
56. O. Mahian, A. Kianifar, S. A. Kalogirou, I. Pop, and S. Wongwises, *Int. J. Heat Mass Transfer* 57, 582 (**2013**).

REVIEW

57. A. J. Chamkha and A. M. Aly, *Chem. Eng. Commun.* 198, 425 **(2011)**.
58. A. J. Chamkha, A. M. Rashad, and E. Al-Meshaiei, *International Journal of Chemical Reactor Engineering* 9, A113 **(2011)**.
59. R. Kandasamy, P. Loganathan, and P. P. Arasu, *Nucl. Eng. Des.* 241, 2053 **(2011)**.
60. B. Ghasemi, S. M. Aminossadati, and A. Raisi, *International Journal of Thermal Sciences* 50, 1748 **(2011)**.
61. M. A. A. Hamad, I. Pop, and A. I. Md Ismail, *Nonlinear Analysis: Real World Applications* 12, 1338 **(2011)**.
62. M. Sheikholeslam, M. Gorji-Bandpay, and D. D. Ganji, *International Communications in Heat and Mass Transfer* 39, 978 **(2012)**.
63. M. Sheikholeslami, M. Gorji-Bandpy, D. D. Ganji, S. Soleimani, and S. M. Seyyedi, *International Communications in Heat and Mass Transfer* 39, 1435 **(2012)**.
64. G. H. R. Kefayati, *International Communications in Heat and Mass Transfer* 40, 67 **(2013)**.
65. G. H. R. Kefayati, *Powder Technol.* 243, 171 **(2013)**.
66. A. H. Mahmoudi, I. Pop, M. Shahi, and F. Talebi, *Computers and Fluids* 72, 46 **(2013)**.
67. W. Ibrahim, B. Shankar, and M. M. Nandeppanavar, *Int. J. Heat Mass Transfer* 56, 1 **(2013)**.
68. M. M. Rashidi, S. Abelman, and N. F. Mehr, *Int. J. Heat Mass Transfer* 62, 515 **(2013)**.
69. O. D. Makinde, W. A. Khan, and Z. H. Khan, *Int. J. Heat Mass Transfer* 62, 526 **(2013)**.
70. O. Mahian, I. Pop, A. Z. Sahin, H. F. Oztop, and S. Wongwises, *Int. J. Heat Mass Transfer* 64, 671 **(2013)**.
71. S. K. Nandy and T. R. Mahapatra, *Int. J. Heat Mass Transfer* 64, 1091 **(2013)**.
72. S. K. Jena and S. K. Mahapatra, *Applied Mathematical Modelling* 37, 527 **(2013)**.
73. M. Sheikholeslami, M. Hatami, and D. D. Ganji, *Powder Technol.* 246, 327 **(2013)**.
74. M. Sheikholeslami, M. Gorji-Bandpy, D. D. Ganji, and S. Soleimani, *Adv. Powder Technol.* 24, 980 **(2013)**.
75. P. V. Murthy, C. RamReddy, A. J. Chamkha, and A. M. Rashad, *International Communications in Heat and Mass Transfer* 47, 41 **(2013)**.
76. A. H. Mahmoudi, I. Mejri, M. A. Abbassi, and A. Omri, *Powder Technol.* 256, 257 **(2014)**.
77. I. Mejri, A. Mahmoudi, M. A. Abbassi, and A. Omri, *Powder Technol.* 266, 340 **(2014)**.
78. M. Sheikholeslami and D. D. Ganji, *Powder Technol.* 253, 789 **(2014)**.
79. M. Sheikholeslami, M. Gorji-Bandpy, and D. D. Ganji, *Powder Technol.* 254, 82 **(2014)**.
80. M. Sheikholeslami, M. Gorji-Bandpy, D. D. Ganji, P. Rana, and S. Soleimani, *Computers and Fluids* 94, 147 **(2014)**.
81. M. Sheikholeslami, M. Hatami, and D. D. Ganji, *J. Mol. Liq.* 190, 112 **(2014)**.
82. M. Sheikholeslami, M. Gorji-Bandpy, D. D. Ganji, and S. Soleimani, *J. Mol. Liq.* 193, 174 **(2014)**.
83. M. Sheikholeslami, M. Gorji-Bandpy, R. Ellahi, M. Hassan, and S. Soleimani, *J. Magn. Magn. Mater.* 349, 188 **(2014)**.
84. M. Sheikholeslami, M. Gorji-Bandpy, R. Ellahi, and A. Zeeshan, *J. Magn. Magn. Mater.* 369, 69 **(2014)**.
85. M. Sheikholeslami, M. Gorji-Bandpy, D.D. Ganji, and S. Soleimani, *Journal of the Taiwan Institute of Chemical Engineers* 45, 40 **(2014)**.
86. A. J. Chamkha and A. M. Rashad, *Computational Thermal Sciences* 6, 27 **(2014)**.
87. A. J. Chamkha, A. M. Rashad, Ch. RamReddy, and P. V. Murthy, *Special Topics and Reviews in Porous Media* 5, 27 **(2014)**.
88. Z. Mehrez, A. El Cafsi, A. Belghith, and P. Le Quéré, *J. Magn. Magn. Mater.* 374, 214 **(2015)**.
89. M. Sheikholeslami, D. D. Ganji, M. Y. Javed, and R. Ellahi, *J. Magn. Magn. Mater.* 374, 36 **(2015)**.
90. M. Sheikholeslami and D. D. Ganji, *Physica A* 417, 273 **(2015)**.
91. B. J. Gireesha, A. J. Chamkha, N. G. Rudraswamy, and M. R. Krishnamurthy, *J. Nanofluids* 4, 66 **(2015)**.

REVIEW